

# Estimation and Stochastic Control of Nonlinear Dynamic Systems over the AWGN Channel: Application in Tele-presence and Tele-operation of Autonomous Vehicles

Somayeh Dolatkhah Takloo, Alireza Farhadi and Ali Khaki-Sedigh

**Abstract**—This paper is concerned with tele-presence and tele-operation of autonomous vehicles over the Additive White Gaussian Noise (AWGN) channel. This wireless communication channel is subject to transmission noise and transmission power constraint. We propose an encoder, decoder and controller by implementing a novel linearization method for linearizing the nonlinear dynamic systems at operating points. For the linearized systems, we implement the encoder, decoder and controller that we previously proposed for output tracking as well as stability of linear dynamic systems. We propose two novel linearization methods and we prove their satisfactory performances for output tracking as well as stability of nonlinear dynamic system. The first method is based on the fixed linearization rate and the second one is based on the variable (optimal) linearization rate. The decoder that is based on the second method is in fact the extended Kalman filter with the optimal linearization rate. We compare the performances of these two methods with each other and the other proposed methods by implementing them to the problems of the tele-presence and tele-operation of autonomous vehicles over the AWGN channel. We illustrate their satisfactory performances. It is illustrated that the second method has higher computational complexity with slightly better performance and is applicable to a larger class of reference trajectories.

**Index Terms** - Networked control system, tele-presence, tele-operation, autonomous vehicle, the unicycle model, the Monte Carlo method.

## I. INTRODUCTION

### A. Motivation and Background

Estimation and stochastic control of dynamic systems over communication channels subject to imperfections are an active research direction in recent years. Communication links in these problems suffer from transmission noise, power constraint, distortion, delay and limited bandwidth and these imperfections make the problem of estimation and control of dynamic systems over communication channel different from the classical estimation and control problems. Examples of remotely controlled systems are the emerging connected and autonomous vehicles, such as unmanned aerial vehicles, autonomous underwater vehicles, e.g., Ifremer's Autonomous Underwater Vehicles (AUVs) [1] and autonomous road vehicles, e.g., Zoox's robotaxis. These emerging systems will have applications in Industry 4.0, military, public transportation, space and underwater exploration, smart agriculture, etc.

S. Dolatkhah Takloo is PhD student in the Department of Electrical and Computer Engineering, K. N. Toosi University of Technology. Email: somayeh.dolatkhah@email.kntu.ac.ir

A. Farhadi is Associate Professor in the Department of Electrical Engineering, Sharif University of Technology. Email: afarhadi@sharif.edu

A. Khaki-Sedigh is Professor in the Department of Electrical and Computer Engineering, K. N. Toosi University of Technology. Email: sedigh@kntu.ac.ir

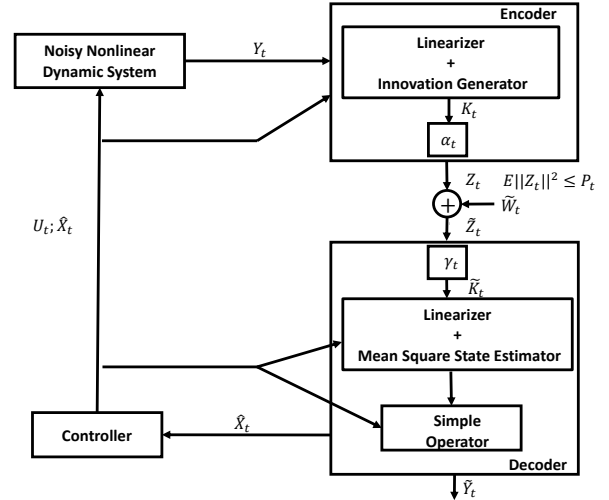


Fig. 1. A nonlinear noisy dynamic system controlled over AWGN channel

For example, Ifremer's AUVs are used for the localization of chemical pollution with unknown location. Remotely controlled road vehicles can be used to transfer front line war wounded to a safe location, in emerging connected vehicles technology, which is the backbone of smart transportation systems, we have vehicle to vehicle wireless communication and vehicle to infrastructure communication, where measured data from vehicle is transmitted subject to imperfections [2], etc. These remotely controlled autonomous vehicles are monitored and controlled real time by distant operator for the intervention in the case of emergency. However, real time monitoring and control over wireless communication links are challenging due to the existence of the communication imperfections, as mentioned above. The focus on the most of tele-operated research papers has been on the communication delay, e.g., [3] - [8]. Nevertheless, the aforementioned tele-operated systems are mainly subject to other types of imperfections, such as noise, limited transmission power/bit rate constraint and rate distortion. Hence, in this paper we focus on communication channels subject to noise and limited transmission power. The monitoring and control of linear dynamic systems over communication links subject to above imperfections have been studied in the literature (e.g., [9]-[14]). However, many practical systems, such as connected and autonomous vehicles have nonlinear dynamics. Hence, nonlinear control over communication channel subject to imperfections is an active research

direction in recent years [1], [15]-[20]. Fig. 1 illustrates a basic block diagram for control over the AWGN channel that has been considered in many papers (e.g., [9] - [11], [13],[14]).

The block diagram of Fig. 1 corresponds to the tele-operation system of autonomous vehicles (e.g., autonomous under water, autonomous road or unmanned aerial vehicles) over the AWGN channel. Miniature unmanned aerial vehicles, for example, are small vehicles controlled remotely by a distant controller/operator. These vehicles are mostly used for aerial photography, shipping and delivering, geographical mapping, disaster management, precision agriculture, search and rescue missions, wildlife monitoring, etc. In the tele-operation of a miniature unmanned aerial vehicle, remote autonomous vehicle should track a desired reference trajectory generated by a distant controller or operator based on the information received from remote vehicle via a wireless channel. High level control signal generated by remote operator should be also sent through wireless communication channel to remote vehicle. Because the remote operator may have access to high power resources for transmission, generated high level control signal can be communicated to the remote vehicle with high transmission power; and hence with high signal to noise ratio and therefore almost without imperfections. However, as the vehicle is small and has limited capacity on-board batteries, the communication from the vehicle to the remote operator should be with the minimum possible transmission power; and therefore, the signal to noise ratio in the path from vehicle to distant controller/operator is low resulting in imperfections in this path, as shown in Fig. 1. Thus, proper encoder and decoder should be designed for the compensation of the noise effects, that unlike the conventional coding scheme, result in real time reliable communication from the dynamic system (i.e., an information source with memory) [16]. The basic block diagram of Fig. 1 can also correspond to the tele-operation problem of AUVs [1]. Sonar wave is used for the underwater wireless communication. Unlike the sea-surface, the deep-sea is silent resulting in high signal to noise ratio in communication from remote controller located in the surface vessel to the remotely operated AUV; and hence, the communication from remote controller/operator to vehicle is almost without imperfections; while the communication from AUV to remote controller is subject to imperfections, as shown in Fig. 1.

The Additive White Gaussian Noise (AWGN) channel considered in the basic block diagram of Fig. 1 is a basic model for wireless communication. This channel is a basic model for satellite communication, deep space communication and when the line of sight is strong. The transmission of information via the AWGN channel is subject to transmission noise and also antenna's power constraint. The output of dynamic system is continuous alphabet with memory. Also the AWGN channel's input and output are continuous alphabet. Thus, the AWGN channel is a suitable communication channel for the remote control of dynamic systems over wireless communication channels. Another motivation for considering the AWGN channel, is the availability of relatively cheap with long communication range FM transceivers [16].

Reference tracking (tele-operation) and tele-presence are the

two main goals in connected vehicles and remotely controlled autonomous vehicles. Reference tracking means the tracking of a desired trajectory designed by a remote human operator/intelligent control unit; and tele-presence means providing the states of remotely controlled vehicle for remote human operator/intelligent control unit in real time so that remote human operator/intelligent control unit is able to design proper desired trajectory for the satisfactory remote reference tracking. Most of papers in this area are concerned with the stability and state tracking of linear dynamic systems at the end of AWGN channel, e.g., [9] - [11], [13],[14]. In [9], the authors presented an optimal control technique for asymptotic bounded mean square stability of a partially observed linear Gaussian system over the AWGN channel. In [13], the authors considered a framework for the feedback stabilization of an open loop unstable linear dynamic system via an AWGN channel subject to limited signal to noise ratio. In [14], the authors investigated stabilization and performance issues for Multi Input-Multi Output (MIMO) linear time invariant system over a MIMO communication link modelled as a parallel AWGN channel. [18] and [21] addressed the problems of controlling of nonlinear dynamic systems over the AWGN channel. [18] presented a novel method based on the describing function for controlling those continuous time dynamics that have periodic outputs to sinusoidal inputs. It also illustrated an application of the theoretical developments in remote control of the unicycle model, which is an abstract model for the autonomous vehicle over the analog AWGN channel. Note that we are living in digital era and therefore analog communication is not widely used. The discrete time dynamic system over the discrete time communication channel, as shown in the block diagram of Fig. 1 is more suitable for today's digital era. Unlike [18] that is concerned with a specific class of dynamic systems, [21] addressed the problem of state tracking of a quite general class of noiseless nonlinear dynamic systems over the AWGN channel and the packet erasure channel. In [22] the authors presented a novel method that is based on the linearization technique [23] with variable and optimal linearization rate and addressed the problems of state tracking, reference tracking and stability of a quite general form of noiseless nonlinear dynamic systems over the packet erasure channel, which is an abstract model for communication via WiFi, the Internet and Zigbee modules.

## B. Paper Contributions

This paper aims to fill the gap in the literature by addressing the problems of state tracking as well as reference tracking of a quite general form of the discrete time nonlinear noisy dynamic system subject to both process and measurement noises over the discrete time AWGN channel, with applications in the tele-presence and tele-operation of autonomous vehicles.

The major contributions of this paper are as follows:

- The extension of the classical linearization method for controlling nonlinear dynamic systems to the context of networked control system for controlling nonlinear systems over the AWGN channel.

- Two different novel linearization methods, namely linearization with fixed rate and variable rate are proposed. In the fixed rate method, the linearization period is fixed and determined so that the stability of the switching system resulted from the linearization is satisfied [16]. The variable rate linearization method is based on the state estimation error. In this method not only the stability of the switching systems is satisfied; but also the upper bound for the linearization period is extracted by monitoring the evolution of the mean square estimation error. Because encoder does not have access to the exact estimation error, and encoder and decoder should agree on a same operating point, the estimation error should be approximated in both encoder and decoder by the Monte Carlo approximation. Once the trend of the mean square estimation error changes, the new linearization is applied. After that in each linearization interval, the available linear networked control methods are used for state as well as reference tracking. The stability of linear switching system which is resulted from linearizing the nonlinear system is shown.
- Proper encoder, decoder and controller are presented for mean square state tracking at the end of communication link as well as reference tracking and stability of nonlinear dynamic systems, when measurements are sent through the AWGN channel.
- The decoder for the case of the linearization with the variable rate is the extended Kalman filter [24] with the optimal linearization rate. To the best of our knowledge, the extended Kalman filter with the optimal linearization rate has not been presented in the literature; and this is another major contributions of this paper.
- The satisfactory performance of the theoretical developments is illustrated via computer simulations by applying the proposed encoder, decoder and controller on the unicycle model, which is an abstract representation for the autonomous vehicles dynamics [1]. It is illustrated that the linearization method with variable rate has higher computational complexity; but it results in a slightly better performance and is applicable to a larger class of reference trajectories.

### C. Paper Organization

The paper is organized as follows. The problem formulation is given in Section II, ; In Section III the design of proper encoder, decoder and controller for tracking of the state trajectories, reference tracking and stability of nonlinear noisy dynamic systems over the AWGN channel is presented. Section IV is devoted to the simulation results for the unicycle model ; and Section V concludes the paper and summarizes the main contributions of the paper and future research directions.

## II. PROBLEM FORMULATION

The following notations are used throughout the paper: The expected value of random variables and the absolute value are denoted by  $E[\cdot]$  and  $|\cdot|$ , respectively.  $\|\cdot\|$  is the Euclidean norm and  $V^{tr}$  denotes the transpose of vector/matrix  $V$ .  $A^{-1}$  and  $\lambda_i(A)$  denote the inverse and eigenvalues of the square matrix  $A$ , respectively.  $\mathbb{R}$  and  $\mathbb{N}$  denote the sets of real numbers and natural numbers, respectively; and  $I_n$  is the identity matrix with dimension  $n \times n$ . Also,  $X^{(i)}$  denotes the  $i$ th element of the vector  $X$  and  $\underline{0}$  denotes the zero vector/matrix.  $\mathbb{R}^+$  is the set of non-negative real numbers and  $\mathbb{N}^+$  is the set of non-negative integers.  $N(m, Q)$  denotes Gaussian distribution with mean  $m$  and variance  $Q$ .  $diag\{ \}$  denotes the diagonal matrix and  $trac()$  denotes the trace of a square matrix.

In this paper we are concerned with the mean square tracking of the state trajectory as well as reference tracking and the stability of discrete time noisy nonlinear dynamic systems over the discrete time AWGN channel, as it is seen in the block diagram of Fig.1. The building blocks of Fig.1 are described below.

**Noisy nonlinear dynamic system:** Noisy nonlinear dynamic system is described by the following dynamic:

$$\begin{cases} X_{t+1} = F(X_t, U_t) + \epsilon_t \\ Y_t = H(X_t) + e_t \end{cases} \quad (1)$$

In the above dynamic system,  $t \in \mathbb{N}^+$  is the time instant,  $F(X_t, U_t) \in \mathbb{R}^n$  is a smooth nonlinear vector of state variables  $X_t$ .  $X_t \in \mathbb{R}^n$ ,  $U_t \in \mathbb{R}^m$  and  $Y_t \in \mathbb{R}^l$  denote the state variables, the control vector and the observation vector at time  $t$ , respectively.  $H(X_t) \in \mathbb{R}^l$  is a smooth nonlinear vector of state variables  $X_t$ . It is also assumed that the initial state  $X_0$  is a Gaussian distributed random variable with mean  $\bar{X}_0$  and variance  $Q_0$  (i.e.,  $X_0 \sim N(\bar{X}_0, Q_0)$ ).  $\epsilon_t$  and  $e_t$  are  $\mathbb{R}^n$ ,  $\mathbb{R}^l$  valued zero mean i.i.d. Gaussian random process and measurement noise with variance  $Q$  and  $R$ , respectively.  $X_0$ ,  $\epsilon_t$  and  $e_t$  are mutually independent.

**Communication Channel:** A parallel discrete time AWGN channel with feedback acknowledgements is considered between dynamic system and controller. It is subject to input power constraint:  $E\|Z_t^{(i)}\|^2 \leq P_t^{(i)}$ ,  $i = 1, 2, \dots, l$ , where  $P_t^{(i)}$  is the transmission power of the  $i$ th antenna and  $Z_t^{(i)}$  is the  $i$ th element of the channel input vector  $Z_t \in \mathbb{R}^l$ . The AWGN channel output is described by  $\tilde{Z}^t = Z_t + \tilde{W}_t$ , where  $\tilde{W}_t$  is zero-mean Gaussian process.

**Encoder:** Encoder is a causal operator denoted by  $Z_t = \mathcal{E}(Y_t, \tilde{Z}^{t-1}, U^{t-1})$  that maps the observation signal vector  $Y_t$  to the channel input  $Z_t$  by the knowledge of the past channel outputs  $\tilde{Z}^{t-1} = (\tilde{Z}_0, \tilde{Z}_1, \dots, \tilde{Z}_{t-1})$  (available for the encoder via the feedback channel) and past control signal vectors  $U^{t-1} = (U_0, U_1, \dots, U_{t-1})$ .

**Decoder:** A Kalman filter which estimates the state vector of systems using channel output and control vector. That is,  $\hat{X}_t = \mathcal{D}(\tilde{Z}^{t-1}, U^{t-1})$  that maps the past channel outputs  $\tilde{Z}^{t-1}$  and the past control signals vectors  $U^{t-1}$  to the system state estimation  $\hat{X}_t$ .

**Controller:** Controller has the following form:  $U_t = U_{[j]} - L_t \Delta \hat{X}_t + \mu_t$ , where  $U_{[j]}$  is the control vector at the  $j$ th oper-

ating point,  $L_t$  is the controller gain, and  $\Delta\hat{X}_t = \Delta\hat{X}_t - R_t$  (where  $R_t$  is the desired reference trajectory vector and  $\Delta\hat{X}_t$  will be determined shortly) and  $\mu_t$  is used for the reference tracking, which will be defined in the next section.

The objective of this paper is to design an encoder, decoder and a controller that result in mean square error in state trajectory tracking, stability and mean square reference tracking of the system (1), as defined below:

*Definition 2.1:* (Mean square error in state trajectory tracking): Consider the block diagram as shown in Fig. 1 described by a noisy nonlinear dynamic (1) over the AWGN channel. It is said that the state trajectory is tracked in the mean square sense if and only if there exist an encoder and a decoder such that for a given  $D_{com} \in \mathbb{R}^+$ , the following property holds for all  $t \in \mathbb{N}^+$ :  $E \left\| X_t - \hat{X}_t \right\|^2 \leq D_{com}$ .

*Definition 2.2:* (Mean square error reference tracking): Consider the block diagram as shown in Fig. 1 described by a noisy nonlinear dynamic (1) over the AWGN channel. It is said that the reference trajectory  $R_t$  is tracked in the mean square sense if and only if there exist an encoder, decoder and a controller such that for a given  $D_c \in \mathbb{R}^+$  the following property holds for all  $t \in \mathbb{N}^+$ :  $E \left\| X_t - R_t \right\|^2 \leq D_c$ .

*Definition 2.3:* (Mean square stability): The stability is a special case of the reference tracking with  $R_t = \underline{0}$

### III. ENCODER, DECODER AND CONTROLLER FOR THE STATE TRACKING, REFERENCE TRACKING AND STABILITY

This section presents a proper encoder, decoder and controller which result in mean square tracking of state trajectory, mean square reference tracking and stability as defined in Definitions 2.1, 2.2 and 2.3. In order to address these problems, we use the linearization method. That is, we linearize the nonlinear dynamic system (1) at operating points with a fixed rate and later on with a variable (optimal) rate and for each linearized system we use the encoder and decoder of [9] that result in output tracking of the partially observed linear dynamic systems subject to Gaussian process and measurement noises over single input - single output AWGN channel. For the simplicity of understanding the proposed coding scheme and controller for the state tracking as well as the reference tracking of the nonlinear dynamic system (1) over the AWGN channel, we first describe the encoder, decoder and controller of [9] for output tracking and stability of linear dynamic systems over the AWGN channel. We then combine this coding scheme with the linearization method to achieve the state tracking, reference tracking and stability of noisy nonlinear dynamic system (1) over the AWGN channel.

#### A. Encoder, Decoder and Controller for the Output Tracking and Stability of Linear Systems over the AWGN Channel

This subsection describes the encoder, decoder and controller of [9]. In [9] the authors studied the mean square asymptotic output tracking and stability of the networked control system of Fig. 1. The system considered here is the partially observed linear dynamic system subject to Gaussian

process and measurement noises over the single input - single output discrete time AWGN channel.

$$\begin{cases} X_{t+1} = AX_t + BU_t + N\epsilon_t, & X_0 = X \\ Y_t = CX_t + De_t \end{cases} \quad (2)$$

In (2),  $X_t \in \mathbb{R}^n$  is the states vector,  $Y_t \in \mathbb{R}$  is the measured output vector and  $U_t \in \mathbb{R}^m$  is the control input vector.  $\epsilon_t \in \mathbb{R}^o$  and  $e_t \in \mathbb{R}^q$  are Gaussian process and measurement noises, respectively. They are i.i.d. zero mean Gaussian with the variance matrices of  $Q$  and  $R$ , respectively. Moreover,  $X \sim N(\bar{X}_0, Q_0)$ ; and  $X$ ,  $\epsilon_t$  and  $V_t$  are mutually independent.

The mean square asymptotic output tracking of [9] is defined as follows:

*Definition 3.1:* (Mean square asymptotic tracking of the output trajectory): Consider the linear dynamic system (2) over the AWGN channel. It is said that the output trajectory is mean square asymptotically tracked at the end of communication channel if and only if there exist an encoder and a decoder such that for a given  $D_v \in \mathbb{R}^+$ , the following property holds:  $\lim_{t \rightarrow \infty} E \left\| Y_t - \tilde{Y}_t \right\|^2 \leq D_v$ , where  $\tilde{Y}_t$  is the reconstruction of  $Y_t$  at the end of communication channel.

For this system over the single input - single output discrete time AWGN channel, the encoder, decoder and controller that result in the mean square asymptotic output tracking and stability are described below:

*Encoder Description:* The linearizer block in Fig. 1 is the identity operator. The innovation generator has the following description ( $\alpha_t$  is defined shortly):

$$Z_t = \alpha_t K_t, \quad K_t = Y_t - \hat{Y}_t, \quad \hat{Y}_t = C\hat{X}_t \quad (3)$$

*Decoder Description:* The linearizer block is the identity operator; and the pre-decoding part (i.e.,  $\tilde{K}_t$ ) is described by

$$\tilde{K}_t = \gamma_t \tilde{Z}_t, \quad (4)$$

where  $\tilde{Z}_t$  is the channel output and  $\alpha_t, \gamma_t \in \mathbb{R}^+$  are defined as follows:

$$\alpha_t = \sqrt{\frac{\eta_t W_C}{D_\nu}}, \quad \gamma_t = \sqrt{\frac{D_\nu \eta_t}{W_C}}, \quad \eta_t = 1 - \frac{D_\nu}{\psi_t}, \quad D_\nu < \min_{t \in \mathbb{N}^+} \psi_t, \quad (5)$$

where  $\psi_t$  will be defined shortly.

*Remark 3.2:* As clarified in [9], the parameters  $\alpha_t$  and  $\gamma_t$  are chosen so that the channel input  $K_t$  is matched to the communication channel resulting in real time reliable communication up to the given distortion level  $D_\nu$ , i.e.,  $E \left\| K_t - \tilde{K}_t \right\|^2 \leq D_\nu$ .

The mean square state estimator has the following description:

$$\begin{aligned} \hat{X}_{t+1} &= A\hat{X}_t + \frac{1}{\alpha_t \gamma_t} A \Pi_t C^{tr} (C \Pi_t C^{tr} + D R D^{tr} + \frac{W_C}{\alpha_t^2})^{-1} \tilde{K}_t \\ &+ B U_t, \quad \hat{X}_0 = \bar{x}_0 = E[X_0], \end{aligned} \quad (6)$$

where  $\Pi_t$  is the mean square state estimation error given by the following Riccati equation:

$$\begin{aligned} \Pi_{t+1} &= A\Pi_t A^{tr} - A\Pi_t C^{tr} (C\Pi_t C^{tr} + DRD^{tr} + \frac{W_C}{\alpha_t^2})^{-1} \\ &C\Pi_t A^{tr} + NQN^{tr}, \Pi_0 = \bar{V}_0 \end{aligned} \quad (7)$$

Then,  $\Psi_t \triangleq C\Pi_t C^{tr} + DRD^{tr}$ . Note that  $\tilde{Y}_t = \tilde{K}_t + C\hat{X}_t$ . It has been shown in [9] that using this coding scheme, we have real time reliable communication up to the distortion level  $D_\nu$ , as follows:  $E\|Y_t - \tilde{Y}_t\|^2 = E\|K_t - \tilde{K}_t\|^2 = D_\nu, \forall t \in \mathbb{N}^+$ . In order to achieve this real time reliable communication by allocating the minimum channel capacity (bandwidth), we should tune the antenna's power as follows:

$$E[Z_t^2] = \alpha_t^2 \Psi_t = \frac{\eta_t W_C}{D_\nu} \Psi_t \triangleq P_t. \quad (8)$$

*Controller Description:* With the assumptions that the pair  $((C^{tr}C, A))$  is detectable and the pair  $(A, B)$  is stabilizable, the stabilizing remote controller that also optimize the following quadratic cost functional

$$\lim_{T \rightarrow \infty} \frac{1}{T} \sum_{t=0}^{T-1} E[\|X_t\|_{C^{tr}C}^2 + \|U_t\|_H^2] \quad (H > 0) \quad (9)$$

is given by

$$U_t = -\Delta_c \hat{X}_t, \quad (10)$$

where  $\Delta_c = (H + B^{tr}P_\infty B)^{-1} B^{tr}P_\infty A$  and  $P_\infty$  is the unique positive semi-definite solution of the following algebraic Riccati equation:

$$P_\infty = AP_\infty A^{tr} - A^{tr}P_\infty B(H + B^{tr}P_\infty B)^{-1} B^{tr}P_\infty A + C^{tr}C. \quad (11)$$

*B. Encoder, Decoder and Controller for the State Tracking, Reference Tracking and Stability of Nonlinear Systems over the AWGN Channel*

In this section, an encoder, decoder and controller for the mean square state tracking as well as the reference tracking and the stability of noisy nonlinear dynamic systems over the AWGN channel are presented.

The applied methodology is based on the linearization of nonlinear noisy dynamic system at operating points, as follows: In the beginning, the nonlinear dynamic is linearized at the initial state  $(\bar{X}_0, U_0), (U_0 = \underline{0})$ . Then the coding scheme presented in Section III-A is applied to the extracted linear model in each sampling time. For each element of the measurement vector of the dynamic system (1), we use the coding scheme of Section III-A. The linearized model is a good approximation of the nonlinear dynamic (1) in the beginning; and therefore, The mean square estimation error, i.e.,  $E\|X_t - \hat{X}_t\|^2$  decreases as time progresses; because the decoder receives more measurements from the dynamic system. But, as time progresses, the nonlinear dynamic system should be linearized at new operating point so that

the best approximation of nonlinear system is available at all time. Throughout, we implement two methods for updating the linearized system: Linearization with fixed rate and linearization with variable (optimal) rate. When the first method is implemented, the time interval of linearization is considered to be fixed. But, when we implement the second method, it is variable. For both methods, there is a lower bound on the linearization period. Beyond this lower bound we may encounter a combination of subsystems which leads to instability of switching systems in [25]. For the second method, we choose the largest possible linearization period that results in a good approximation of the nonlinear system by the family of the linearized systems.

In [25] the stability is shown by determining linearization period under the dwell time  $\tau_a$ . It is shown in [26] that the average dwell time  $\tau_a$ , which is a measure of the frequency of switches (here the frequency of updating linearized system), should be greater than or equal to a critical value denoted by  $\tau_a^*$  defined as follows.  $\tau_a \geq \tau_a^*$ ;  $\tau_a = \frac{t}{N_t}$ ;  $\tau_a^* = \frac{\ln h}{\ln \lambda - \ln \lambda^*}$ , where  $N_t$  is the number of switches that occurs in the time interval of  $[0, t]$  and  $h, \lambda$  and  $\lambda^*$  are defined as follows:

For all linearized models with the system matrix  $A_{[j]}$ , there exist  $\lambda_1 < 1$  and  $\lambda_2 > 1$  such that the following relations hold [26]:  $\|A_{[j]}\| < 1$ ;  $\|A_{[j]}^t\| \leq h_j \lambda_1^t$ , where  $\|A_{[j]}\| \geq 1$ ;  $\|A_{[j]}^t\| \leq h_j \lambda_2^t$ . Then,  $h = \max_j h_j$ ,  $\lambda \in [\lambda_1, 1]$  and  $\lambda^* \in [\lambda_1, \lambda]$  is the largest value that satisfies the following inequality for some  $c > 0$ :  $\|X_t\| \leq c(\lambda^*)^t \|X_0\|$ . In order to satisfy the above condition, it is sufficient that the linearization period  $T_l$  is much larger than the system sampling period (e.g.,  $T_l \geq 15T$ , where  $T$  is the sampling period).

*1) Encoder, Decoder and Controller Descriptions for the Fixed as well as Variable Linearization Rates:* Suppose for  $j \in \mathbb{N}$  the  $j$ th linearized system, which is obtained by linearizing the nonlinear dynamic system (1) at the current operating point  $(X_{[j]}, U_{[j]})$ , has the following description (Note that  $(X_{[1]}, U_{[1]}) = (\bar{X}_0, U_0)$ ,  $(X_{[2]}, U_{[2]}) = (\hat{X}_{T_l}, U_{T_l})$ , etc.):

$$\begin{cases} \Delta X_{t+1} = A_{[j]} \Delta X_t + B_{[j]} \Delta U_t + \epsilon_t \\ \Delta Y_t = C_{[j]} \Delta X_t + e_t \\ t = \{(j-1)T_l, \dots, jT_l - 1\}, \end{cases} \quad (12)$$

where  $A_{[j]} = \frac{\partial F}{\partial X}|_{(X_{[j]}, U_{[j]})}$ ,  $B_{[j]} = \frac{\partial F}{\partial U}|_{(X_{[j]}, U_{[j]})}$ ,  $C_{[j]} = \frac{\partial H}{\partial X}|_{(X_{[j]}, U_{[j]})}$ ,  $\Delta X_{t+1} = X_{t+1} - F(X_{[j]}, U_{[j]})$ ,  $\Delta X_t = X_t - X_{[j]}$ ,  $\Delta U_t = U_t - U_{[j]}$  and  $\Delta Y_t = Y_t - H(X_{[j]})$ . The encoder and decoder are described in the following:

*Encoder Description:* The linearizer block is described by (12). The innovation generator block for each element of the vector  $Z_t$  has the following description:

$$\begin{aligned} Z_t^{(i)} &= \alpha_t^{(i)} K_t^{(i)}, \quad K_t = \Delta Y_t - \Delta \hat{Y}_t, \quad \Delta \hat{Y}_t = C_{[j]} \Delta \hat{X}_t, \\ \Delta \hat{X}_t &= \hat{X}_t - X_{[j]} \end{aligned} \quad (13)$$

*Decoder Description:* The linearizer block is described by (12); and each element of the pre-decoding part (i.e.,  $\tilde{K}_t$ ) is

described by

$$\tilde{K}_t^{(i)} = \gamma_t^{(i)} \tilde{Z}_t^{(i)}, \quad (14)$$

where  $\tilde{Z}_t^{(i)}$  is the channel output and  $\alpha_t^{(i)}, \gamma_t^{(i)} \in \mathbb{R}^+$  are defined as follows:

$$\alpha_t^{(i)} = \sqrt{\frac{\eta_t^{(i)} W_C^{(i)}}{D_\nu}}, \quad \eta_t^{(i)} = 1 - \frac{D_\nu}{\psi_{t,ii}}, \quad \gamma_t^{(i)} = \sqrt{\frac{D_\nu \eta_t^{(i)}}{W_C^{(i)}}},$$

$$D_\nu < \min_{t \in \mathbb{N}^+} \psi_{t,ii}. \quad (15)$$

where  $\psi_{t,ii}$  will be defined shortly. The recursive Kalman filter estimator is then described as follows:

$$\Delta \hat{X}_{t+1} = A_{[j]} \Delta \hat{X}_t + A_{[j]} \Pi_t C_{[j]}^{tr} (C_{[j]} \Pi_t C_{[j]}^{tr} + R + \alpha_t^{-2} W_C)^{-1} (\alpha_t \gamma_t)^{-1} \tilde{K}_t + B_{[j]} \Delta U_t, \quad \Delta \hat{X}_{(j-1)T_l} = 0 \quad (16)$$

where  $\alpha_t = \text{diag}\{\alpha_t^{(1)}, \alpha_t^{(2)}, \dots, \alpha_t^{(l)}\}$ ,  $\gamma_t = \text{diag}\{\gamma_t^{(1)}, \gamma_t^{(2)}, \dots, \gamma_t^{(l)}\}$  and  $\Pi_t$  is the mean square state estimation error variance matrix given by :

$$\Pi_{t+1} = A_{[j]} \Pi_t A_{[j]}^{tr} - A_{[j]} \Pi_t C_{[j]}^{tr} (C_{[j]} \Pi_t C_{[j]}^{tr} + R + \alpha_t^{-2} W_C)^{-1} C_{[j]} \Pi_t A_{[j]}^{tr} + Q. \quad (17)$$

Then,  $\Psi_t = C_{[j]} \Pi_t C_{[j]}^{tr} + R$  and  $\Psi_{t,ii}$  is the  $i$ th diagonal element of the matrix  $\Psi_t$ . Note that for each  $t \in [(j-1)T_l, jT_l-1]$ ,  $\Delta \hat{X}_t = \hat{X}_t - X_{[j]}$  and  $\Delta \tilde{Y}_t = \tilde{K}_t + C_{[j]} \Delta \hat{X}_t$ . It can be shown that using this coding scheme, we have the real time reliable communication up to the distortion level  $lD_\nu$ , as follows:  $E \left\| \Delta Y_t - \Delta \tilde{Y}_t \right\|^2 = E \left\| K_t - \tilde{K}_t \right\|^2 = lD_\nu$ .

In order to achieve this real time reliable communication, we should tune the antenna's power at each linearized zone as follows:

$$E[(Z_t^{(i)})^2] = (\alpha_t^{(i)})^2 \Psi_{t,ii} = \frac{\eta_t^{(i)} W_C^{(i)}}{D_\nu} \Psi_{t,ii} \triangleq P_t^{(i)}. \quad (18)$$

**Controller Description:** The controller is described in the following form as mentioned in Section II  $\Delta U_t = -L_t \Delta \hat{X}_t + \mu_t$ , where  $\Delta \hat{X}_t = \Delta \hat{X}_t - R_t$  and for each  $t \in [(j-1)T_l, jT_l-1]$ ,  $L_t = L_{[j]}$  is chosen such that the matrix  $A_{[j]} - B_{[j]} L_{[j]}$  is stable and  $\mu_t$  is chosen such that  $\mu_t = -B_{[j]}^+ ((A_{[j]} - B_{[j]} L_{[j]})(R_t - X_{[j]}) + B_{[j]} L_{[j]} R_t - R_{t+1} + F(X_{[j]}, U_{[j]}))$ , where  $B_{[j]}^+$  is the pseudo inverse of the matrix  $B_{[j]}$ .

**2) Realization of the Fixed and Variable Linearization Rate Methods:** : The fixed linearization rate method is easily obtained by fixing a linearization period, which is sufficiently larger than the sampling period (e.g.,  $T_l = 15T$ ) and sufficiently small that results in a good approximation of the nonlinear system by the family of the linearized equivalent systems. But, for the variable linearization rate case, the encoder and decoder should agree on the time of linearization. Generally speaking, when the linearized system is getting away from the nonlinear system, the linearization should be

updated. In the beginning of a new linearization zone, the trace of the estimation error,  $\text{trac}(\Pi_t)$  (which is the mean square estimation error) is strictly increasing or decreasing. When the time progresses, this increasing or decreasing trend is violated as the linearized system is getting away from the nonlinear system; and therefore, the time when the increasing or decreasing trend of the mean square estimation error is violated, is the right time for updating the linearized system. Note that the encoder and decoder in the proposed method reconstruct the mean square estimation error using the Monte Carlo approximation method by the knowledge of  $\Delta \hat{X}_t$  communicated to the encoder by the feedback channel. This method works as follows:

At the sample time  $t = 0$ , the encoder and decoder choose  $M$  realization for  $X_0 \sim N(\bar{X}_0, Q_0)$  and computes  $E_0 = \frac{1}{\sqrt{M}} (X_0^{[1]} - \hat{X}_0 \quad \dots \quad X_0^{[M]} - \hat{X}_0)$ , where  $X_0^{[i]}$  is the  $i$ th realization of  $X_0$ . Subsequently,  $\Pi_0 = E_0 E_0^{tr}$ . At the time instant  $t = 1$ , using the description (1) for the nonlinear dynamic system and  $M$  realization obtained for  $X_0$  available from the previous time instant as well as  $M$  realization for the process noise, the encoder and decoder compute  $M$  realization for  $X_1$ . Then, they compute  $E_1 = \frac{1}{\sqrt{M}} (X_1^{[1]} - \hat{X}_1 \quad \dots \quad X_1^{[M]} - \hat{X}_1)$ , where  $X_1^{[i]}$  is the  $i$ th realization of  $X_1$ . Subsequently,  $\Pi_1 = E_1 E_1^{tr}$ . Similarly, for the other time instances,  $\Pi_t$  is reconstructed at the encoder and decoder; and hence, the encoder and decoder by observing the increasing or decreasing trend of  $\text{trace}(\Pi_t)$  determine the right time for updating the linearized system.

**3) Mathematical Proofs:** Now, in the following we show that using the proposed coding scheme and controller, we have the mean square tracking of the state trajectory at the end of communication channel as well as the reference tracking and hence the stability. These results are shown in the following two propositions.

**Proposition 3.3:** (Mean square state tracking): Consider the control/communication block diagram of Fig. 1 described by the nonlinear dynamic system (1) and the proposed coding scheme and controller. For this system we have the mean square state tracking, as defined in Definition 2.1, provided the pair  $(C_{[j]}, A_{[j]})$  is detectable, the pair  $(A_{[j]}, Q^{\frac{1}{2}})$  is stabilizable and the linearization period  $T_l$  is sufficiently small and greater than the sampling period  $T$ .

**Proof:** As the linearization period  $T_l$  is sufficiently small, the linearized system is a good approximation of the nonlinear system. Consequently, at each linearized zone the mean square estimation error tends to the steady state value of the mean square estimation error (i.e.,  $E \left\| X_{[j]} - \hat{X}_{[j]} \right\|^2$ ), which is a bounded value as the pair  $(C_{[j]}, A_{[j]})$  is detectable and the pair  $(A_{[j]}, Q^{\frac{1}{2}})$  is stabilizable [27]. In other words, in each linearized zone, we get an asymptotically bounded estimation; and hence, as the linearization is not too frequent, we get asymptotically bounded estimation for the nonlinear dynamic as it has been proved in the Theorem 3.1 of [28] and [29].

**Remark 3.4:** i) The case of variable linearization period, is

optimal in the sense that in this method the linearized system is updated at the right time when the linearized system starts getting a way from the nonlinear system. In other words, it is the largest linearization period that results in a very good approximation for the nonlinear system by the family of the linearized systems.

ii) The proposed decoder is the extended Kalman filter and for the case with the variable (optimal) linearization rate, it is the extended Kalman filter with the optimal linearization rate. In order to implement this filter to nonlinear systems, we should consider the increasing or decreasing trend of  $\text{trac}(\Pi_t)$  at each linearized zone and update the linearized system when this trend changes. To the best of our knowledge, the extended Kalman filter with the optimal linearization rate has not been presented in the literature.

**Proposition 3.5:** (Mean square error reference tracking and stability): Consider the control/communication block diagram of Fig. 1 described by the nonlinear dynamic system (1) and the proposed coding scheme and controller. For this system, we have the mean square reference tracking and stability, as defined in Definitions 2.2 and 2.3, provided the linearization period is sufficiently small and greater than the sampling period  $T$ , the pair  $(A_{[j]}, B_{[j]})$  is stabilizable, the pair  $(C_{[j]}, A_{[j]})$  is detectable and the pair  $(A_{[j]}, Q^{\frac{1}{2}})$  is stabilizable. *Proof:* Define the reference tracking error, as follows:  $E_t^r = X_t - R_t$ . Therefore, for each  $t \in [(j-1)T_l, jT_l - 1]$  we have the following relations for the state tracking error:

$$\begin{aligned} E_{t+1}^r &= X_{t+1} - R_{t+1} \\ &= (X_{t+1} - F(X_{[j]}, U_{[j]})) + F(X_{[j]}, U_{[j]}) - R_{t+1} \\ &= \Delta X_{t+1} + F(X_{[j]}, U_{[j]}) - R_{t+1} \\ &= A_{[j]}\Delta X_t - B_{[j]}L_{[j]}\Delta \hat{X}_t + B_{[j]}\mu_t + \epsilon_t - R_{t+1} \\ &\quad + F(X_{[j]}, U_{[j]}) \\ &= A_{[j]}\Delta X_t - B_{[j]}L_{[j]}\Delta \hat{X}_t + B_{[j]}L_{[j]}R_t + B_{[j]}\mu_t + \\ &\quad \epsilon_t - R_{t+1} + F(X_{[j]}, U_{[j]}). \end{aligned} \quad (19)$$

Hence, from the above relations, we have  $(E_t = X_t - \hat{X}_t = \Delta X_t - \Delta \hat{X}_t)$ :

$$\begin{aligned} E_{t+1}^r &= A_{[j]}\Delta X_t - B_{[j]}L_{[j]}\Delta X_t + B_{[j]}L_{[j]}E_t + B_{[j]}L_{[j]}R_t \\ &\quad + B_{[j]}\mu_t + \epsilon_t - R_{t+1} + F(X_{[j]}, U_{[j]}) \\ &= (A_{[j]} - B_{[j]}L_{[j]})\Delta X_t + B_{[j]}L_{[j]}E_t + B_{[j]}L_{[j]}R_t \\ &\quad + B_{[j]}\mu_t + \epsilon_t - R_{t+1} + F(X_{[j]}, U_{[j]}). \end{aligned} \quad (20)$$

Recall that  $E_t^r = X_t - R_t$ ; and therefore,  $E_t^r = (X_t - X_{[j]}) + X_{[j]} - R_t = \Delta X_t + X_{[j]} - R_t$ . Hence, from the above relations, we have

$$\begin{aligned} E_{t+1}^r &= (A_{[j]} - B_{[j]}L_{[j]})E_t^r + (A_{[j]} - B_{[j]}L_{[j]})(R_t - X_{[j]}) \\ &\quad + B_{[j]}L_{[j]}E_t + B_{[j]}L_{[j]}R_t + B_{[j]}\mu_t + \epsilon_t - R_{t+1} \\ &\quad + F(X_{[j]}, U_{[j]}). \end{aligned} \quad (21)$$

Now as  $\mu_t = -B_{[j]}^+((A_{[j]} - B_{[j]}L_{[j]})(R_t - X_{[j]}) + B_{[j]}L_{[j]}R_t - R_{t+1} + F(X_{[j]}, U_{[j]}))$ , the above equality for  $E_{t+1}^r$  is approx-

imated by the following:

$$E_{t+1}^r = (A_{[j]} - B_{[j]}L_{[j]})E_t^r + B_{[j]}L_{[j]}E_t + \epsilon_t. \quad (22)$$

Now, for the simplicity of the presentation, suppose that  $\epsilon_t = 0$  (the general case is treated similarly). Therefore, we have:

$$E_{t+1}^r = (A_{[j]} - B_{[j]}L_{[j]})E_t^r + B_{[j]}L_{[j]}E_t. \quad (23)$$

Consequently, from the above recursive equation for  $E_t^r$ , we get the following expression for  $E_t^r$  for the  $j$ th linearized zone (i.e.,  $t \in [(j-1)T_l + 1, jT_l]$ ).

$$\begin{aligned} E_t^r &= (A_{[j]} - B_{[j]}L_{[j]})^{t-(j-1)T_l} E_{(j-1)T_l}^r \\ &\quad + \sum_{k=(j-1)T_l}^{t-1} (A_{[j]} - B_{[j]}L_{[j]})^{t-1-k} B_{[j]}L_{[j]}E_k, \end{aligned} \quad (24)$$

$$t \in [(j-1)T_l + 1, jT_l].$$

Now, as  $E_{(j-1)T_l}^r$  and  $E_k$  are independent and  $E_k$  is also an independent process with zero mean, we get the following expression for  $E[E_t^{r\ tr} E_t^r]$ .

$$\begin{aligned} E[E_t^{r\ tr} E_t^r] &= E[|X_t - R_t|^2] \\ &= ((A_{[j]} - B_{[j]}L_{[j]})^{t-(j-1)T_l})^{tr} (A_{[j]} - B_{[j]}L_{[j]})^{t-(j-1)T_l} \\ &\quad \cdot \text{trac}(E[E_{(j-1)T_l}^r E_{(j-1)T_l}^{r\ tr}]) + \sum_{k=(j-1)T_l}^{t-1} L_{[j]}^{tr} B_{[j]}^{tr} ((A_{[j]} - \\ &\quad B_{[j]}L_{[j]})^{t-1-k})^{tr} (A_{[j]} - B_{[j]}L_{[j]})^{t-1-k} B_{[j]}L_{[j]} \text{trac} \\ &\quad (E[E_k E_k^{tr}]). \end{aligned} \quad (25)$$

Recall that the controller gain  $L_{[j]}$  is chosen so that the matrix  $A_{[j]} - B_{[j]}L_{[j]}$  is a stable matrix. Hence, when  $t \in [(j-1)T_l + 1, jT_l]$  increases, the first term in the above equality tends to zero and hence it remains bounded. In addition, recall that it has been shown in the above proposition that the mean square estimation error decreases and remains bounded as time increases. Therefore, the second term in the above equality also remains bounded as  $t$  increases. Consequently, in each linearized zone the tracking error is mean square bounded (stable); and hence, the combined system remains bounded. This completes the proof for the mean square reference tracking and also mean square stability because the stability is a special case of the reference tracking with  $R_t = \underline{0}$ .

**Remark 3.6:** For each linearized equivalent system, the controller gain  $L_{[j]}$  should be chosen so that the matrix  $A_{[j]} - B_{[j]}L_{[j]}$  is a stable matrix.

#### IV. SIMULATION RESULTS

In order to verify the satisfactory performance of the two proposed linearization methods, we consider the block diagram of Fig. 1 described by the nonlinear dynamic system (27). Presented encoder, decoder and controller will be applied to the unicycle model for remote controlling. The dynamics of miniature drones, autonomous road vehicles and autonomous under water vehicles are described by a 6 degrees of freedom model. However, the vehicle dynamic can be handled by local

control loops, which results in the kinematic unicycle model, as described below [13]:

$$\begin{cases} \dot{x}(t) = v(t) \cos(\theta(t)) \\ \dot{y}(t) = v(t) \sin(\theta(t)) \\ \dot{\theta}(t) = u(t) \end{cases} \quad (26)$$

where  $(x(t), y(t))$  is the vehicle position,  $\theta(t)$  the vehicle orientation,  $v(t)$  is the forward velocity and  $u(t)$  is the rotational velocity. The state vector of the system is  $X(t) = [x(t) \ y(t) \ \theta(t)]^{tr}$  and  $U(t) = [v(t) \ u(t)]^{tr}$  is the control vector. The discrete time equivalent model is (27), where  $T$  is the sampling period.

$$\begin{cases} x_{t+1} = x_t + Tv_t \cos(\theta_t) \\ y_{t+1} = y_t + Tv_t \sin(\theta_t) \\ \theta_{t+1} = \theta_t + Tu_t \end{cases} \quad (27)$$

Note that in (27)  $x_t, y_t, \theta_t, v_t$  and  $u_t$  are the discrete time equivalent signals of  $x(t), y(t), \theta(t), v(t)$  and  $u(t)$ , respectively. Note also that for this model, the state vector is  $X_t = [x_t \ y_t \ \theta_t]^{tr}$ . Consequently, the state space representation of the family of the discrete time equivalent linearized systems, have the following state space matrices:

$$A_{[j]} = \begin{bmatrix} 1 & 0 & -Tv_{[j]} \sin(\theta_{[j]}) \\ 0 & 1 & Tv_{[j]} \cos(\theta_{[j]}) \\ 0 & 0 & 1 \end{bmatrix} \quad (28)$$

$$B_{[j]} = \begin{bmatrix} T \cos(\theta_{[j]}) & 0 \\ T \sin(\theta_{[j]}) & 0 \\ 0 & T \end{bmatrix} \quad (29)$$

Here, the unicycle model should track a circle with center at (5,3) and the radius of 2. Therefore, we choose the reference vector  $R_t = [r_t^{[x]} \ r_t^{[y]} \ r_t^{[\theta]}]^{tr}$ , as follows:

$$\begin{aligned} [r_t^{[x]} \ r_t^{[y]} \ r_t^{[\theta]}]^{tr} &= [5 + 2 \cos(3f_0 t) \ 3 + 2 \sin(3f_0 t) \\ &\quad \arctan\left(\frac{r_t^{[y]} - \hat{y}_{t-1}}{r_t^{[x]} - \hat{x}_{t-1}}\right)]^{tr}. \end{aligned} \quad (30)$$

**Fixed Rate Case:** Now we consider  $f_0 = 10^{-2}$  as reference signal frequency and  $x_0 \sim N(1,1)$ ,  $y_0 \sim N(1,1)$ ,  $\theta_0 \sim N(1,1)$  and we consider a  $3 \times 3$  parallel Gaussian channel with zero mean white Gaussian noise and the identity variance matrix. The system outputs, i.e.,  $x_t, y_t$  and  $\theta_t$ , which are sampled from  $x(t), y(t)$  and  $\theta(t)$  with sampling period  $T$  seconds are sent through this parallel Gaussian channel to the remote controller; and the proper control signals  $u_t$  and  $v_t$  generated by remote controller are applied to the nonlinear dynamic system (26) by a Zero Order Hold (Z.O.H) mechanism. Throughout this section we set  $D_v = 2$ .

Fig. 2-Fig. 6 illustrate that the system outputs track the reference signal when the measurements and system are not subject to noise (i.e.,  $e_t, \epsilon_t \sim N(0,0)$ ) and when  $T = 10^{-2}$  seconds. Note that for this simulation, we fix the linearization period to be  $T=0.15$  seconds. Note also that the critical value for the average dwell time ( $\tau_a^*$ ) for this simulation is 6.3 and considering the discretization with sampling period of  $T_0 = 10^{-2}$  it is  $\tau_a^* = 0.0063$ . Based on the simulation results we can find that, the system outputs  $x_t, y_t$  and  $\theta_t$  eventually track the reference signals  $r_t^{[x]}, r_t^{[y]}$  and  $r_t^{[\theta]}$ . Therefore, as it

is seen in Fig. 6 the autonomous vehicle eventually tracks the desired reference circle. This result is expected from Proposition 3.5 because for the very small sampling period  $T$ , the discrete time equivalent dynamic system (27), which is used for the design of remote controller, is a very good approximation of the actual dynamic of (26).

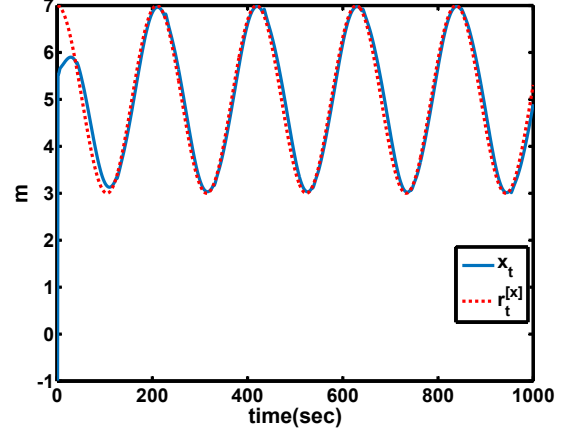


Fig. 2.  $x_t$  and  $r_t^{[x]}$  for the fixed rate linearization method when  $\epsilon_t, e_t \sim N(0,0)$

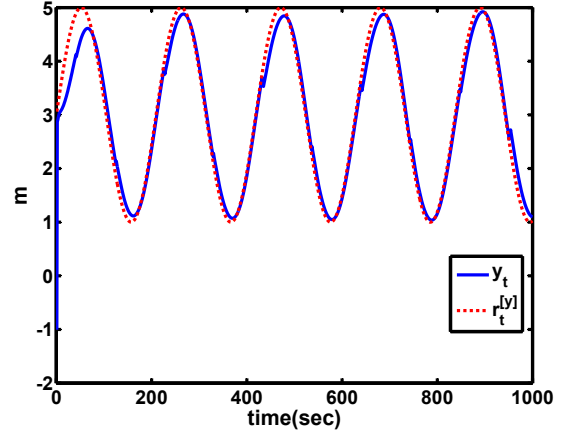


Fig. 3.  $y_t$  and  $r_t^{[y]}$  for the fixed rate linearization method when  $\epsilon_t, e_t \sim N(0,0)$

To illustrate the satisfactory performance of the proposed method in comparison to the classical nonlinear control methods, we apply the presented method on [30] to the block diagram of Fig. 1 described by the unicycle model as the nonlinear dynamic. Fig. 6 illustrates the tracking performance of the proposed method and Fig. 7 illustrates the tracking performance of the feedback linearization method presented in [30]. The classical feedback linearization method has not been designed to deal with the effects of communication imperfections, such as limited transmission power and transmission noise; while our proposed method has been mainly designed to compensate these imperfections. Hence, as it is clear from Fig. 6 and Fig. 7, the proposed method results in much better reference tracking performance. To compare

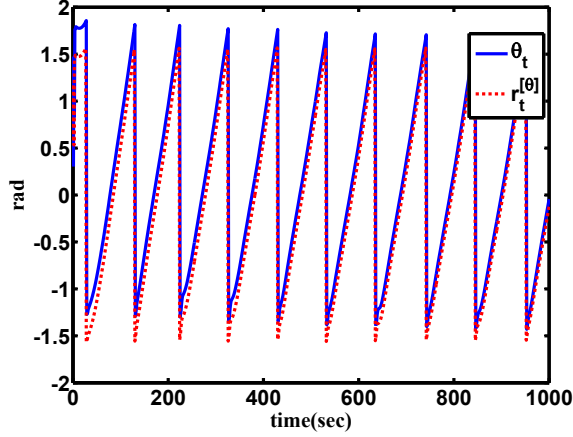


Fig. 4.  $\theta_t$  and  $r_t^{[\theta]}$  for the fixed rate linearization method when  $\epsilon_t, e_t \sim N(0, 0)$

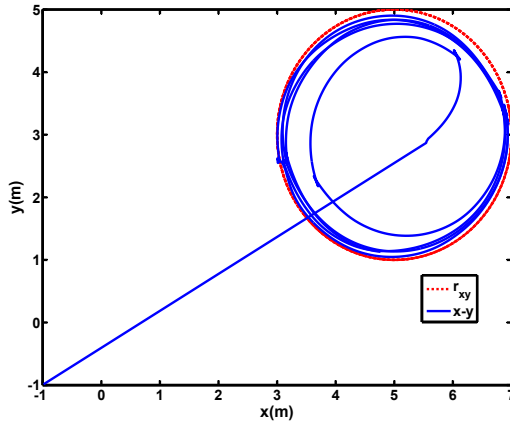


Fig. 5.  $x_t - y_t$  for the fixed rate linearization method when  $\epsilon_t, e_t \sim N(0, 0)$

our proposed method with other similar methods note that in [18] using a novel method, which is based on the describing function, the reference tracking of the unicycle model over the analog AWGN channel was addressed. Comparing the simulation result depicted in Fig. 5 and those depicted in [18] reveals that the performance of the proposed method is as good as the performance of the method presented in [18]. Nevertheless, the proposed method is applicable to much larger class of nonlinear systems and reference trajectories; while the method presented in [18] is only applicable to specific dynamics that have periodic outputs to sinusoidal

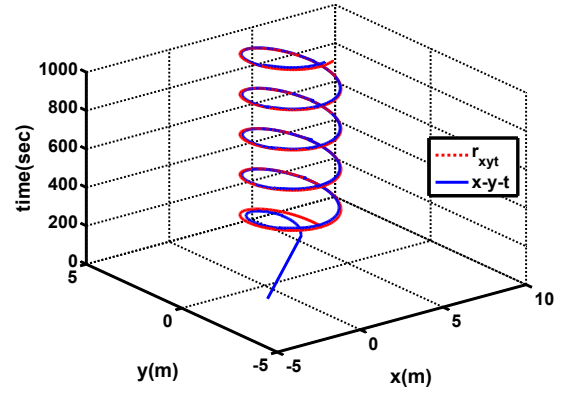


Fig. 6.  $x_t - y_t - t$  for the fixed rate linearization method when  $\epsilon_t, e_t \sim N(0, 0)$

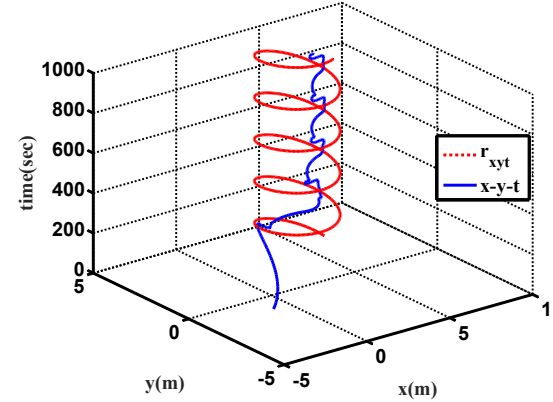


Fig. 7.  $x_t - y_t - t$  for the classical feedback linearization technique when  $\epsilon_t, e_t \sim N(0, 0)$

inputs.

Now to quantify the performance of the proposed method, we define the Root Sum Square Error (RSSE) criterion as follows:  $RSSE =$

$$\sqrt{\sum_{t=\text{start time}}^{\text{end time}} (x_t - r_x^{[t]})^2 + (y_t - r_y^{[t]})^2 + (\theta_t - r_\theta^{[t]})^2}$$

RSSE associated with Fig. 6 which corresponds to the case of zero process and measurement noises for  $t = 0$  to  $t = 10^3$  sec. is 21.7861. For the case of  $\epsilon_t \sim N(0, 0.1.I_3)$  and  $e_t \sim N(0, 0.1.I_3)$ , RSSE is 24.6806. For the case of  $\epsilon_t \sim N(0, I_3)$  and  $e_t \sim N(0, I_3)$ , RSSE is 25.6621. Table I summarizes these computations. This table illustrates that the proposed method is robust against measurement and system noises.

TABLE I  
RSSES COMPUTED FOR DIFFERENT PROCESS AND MEASUREMENT NOISES WHEN THE FIXED RATE LINEARIZATION METHOD IS IMPLEMENTED

Case	RSSE
$\epsilon_t = 0, e_t = 0$	21.7861
$\epsilon_t, e_t \sim N(0, 0.1.I_3)$	24.6806
$\epsilon_t, e_t \sim N(0, I_3)$	25.6621

For the linearization period of 0.15 sec., the RSSE associated with Fig. 6, which corresponds to the case of  $T = 10^{-2}$  sec. for  $t = 0$  to  $t = 10^3$  is 21.7861. For the case of  $T = 10^{-3}$

sec., RSSE is 36.9455. However, as for this case the number of sampled used to compute RSSE is 10 times more than that of used for the other case, we should normalize its RSSE by multiplying 36.9455 by  $\frac{1}{\sqrt{10}}$  to get the normalized RSSE with the value of 11.6832. For the case of  $T = 0.1$  sec. and the linearization period of 0.2 sec., RSSE is 56.8147 and the normalized value is 179.6639. Table II summarizes these computations. This result is expected because for the latter case, the frequency of switching between stable linearized systems is fast; and therefore, the combined system tends to be unstable.

TABLE II  
RSSES COMPUTED FOR DIFFERENT SAMPLE PERIODS WHEN THE FIXED RATE LINEARIZATION METHOD IS IMPLEMENTED

Case	RSSE
T=0.001	11.6832
T=0.01	21.7861
T=0.1	179.6639

Table III compares RSSE for difference channel noise when  $T = 10^{-2}$  seconds, the linearization period is 0.15 seconds and the system is not subject to process and measurement noises. This table illustrates that the proposed method is also robust against channel noise.

TABLE III  
RSSES COMPUTED FOR DIFFERENT CHANNEL NOISES WHEN THE FIXED RATE LINEARIZATION METHOD IS IMPLEMENTED

Case	RSSE
$\tilde{W}_t \sim N(0, 0.1.I_3)$	20.3024
$\tilde{W}_t \sim N(0, I_3)$	21.7861
$\tilde{W}_t \sim N(0, 2.I_3)$	23.6912

**Variable Rate Case:** Now, we repeat the above results when we use the second proposed method, that is, the linearization with the optimal rate to be able to compare these two methods with each other. Fig. 8 is the counterpart of Fig. 6 with the optimal linearization rate. Tables IV, V, VI are also the counterparts of Tables I, II and III, respectively, for the optimal rate case. From these figures and tables it follows that the second method has a slightly better performance, as it is expected although its computational load is much higher than that of the first method.

Now, consider the situation where the autonomous vehicle of the case study should track a much faster reference trajectory. To simulate this situation, we set  $T_0 = 0.1$ . Fig. 9 illustrates the performance of the second method (i.e., the variable rate linearization method). For the first method, we get a very poor performance with the  $RSSE = 46.8422$  and for the second method, we get a good quality performance with the  $RSSE = 17.309$ . Table VII summarizes the  $RSSEs$  for different  $T_0$ . As it is clear from these figure and table, the second method is able to track faster reference signals; while the first method is not able to do that.

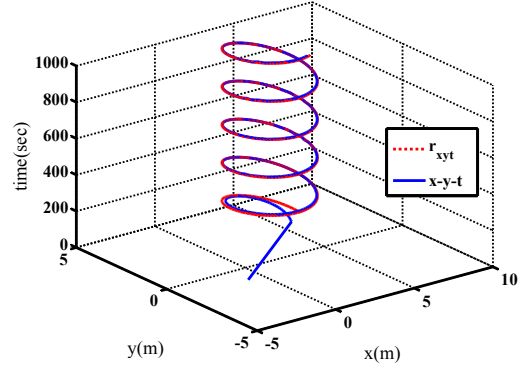


Fig. 8.  $x_t - y_t - t$  for the variable rate linearization method when  $\epsilon_t, e_t \sim N(0, 0)$

TABLE IV  
RSSES COMPUTED FOR DIFFERENT PROCESS AND MEASUREMENT NOISES WHEN THE VARIABLE RATE LINEARIZATION METHOD IS IMPLEMENTED

Case	RSSE
$\epsilon_t = 0, e_t = 0$	20.7421
$\epsilon_t, e_t \sim N(0, 0.1.I_3)$	21.4337
$\epsilon_t, e_t \sim N(0, I_3)$	24.72

TABLE V  
RSSES COMPUTED FOR DIFFERENT SAMPLE PERIODS WHEN THE VARIABLE RATE LINEARIZATION METHOD IS IMPLEMENTED

Case	RSSE
T=0.001	25.6187
T=0.01	20.7421
T=0.1	38.5883

TABLE VI  
RSSES COMPUTED FOR DIFFERENT CHANNEL NOISES WHEN THE VARIABLE RATE LINEARIZATION METHOD IS IMPLEMENTED

Case	RSSE
$\tilde{W}_t \sim N(0, 0.1.I_3)$	18.8167
$\tilde{W}_t \sim N(0, I_3)$	20.7421
$\tilde{W}_t \sim N(0, 2.I_3)$	21.4172

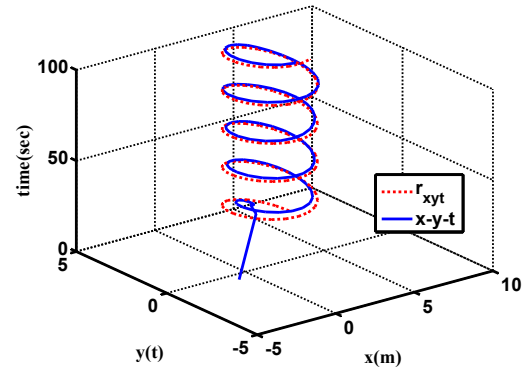


Fig. 9.  $x_t - y_t - t$  for the variable rate linearization method when  $T_0 = 0.1$

## V. CONCLUSION AND DIRECTIONS FOR FUTURE RESEARCH

This paper addressed the problem of mean square state tracking, reference tracking and stability of nonlinear noisy dynamic systems over the AWGN channel with applications in tele-presence and tele-operation of autonomous vehicles. The

TABLE VII  
RSSEs COMPUTED FOR DIFFERENT  $T_0$  WHEN THE VARIABLE RATE  
LINEARIZATION METHOD IS IMPLEMENTED

$T_0$	RSSE
0.1	17.309
0.2	21.5507
0.5	23.5127
1	22.2473

proposed technique was based on the linearization with fixed and variable rates. A proper encoder, decoder and controller for state tracking of nonlinear dynamics at the end of communication channel as well as reference tracking and stability over the AWGN channel were presented. The satisfactory performances of the proposed methods were illustrated by applying them to the unicycle model, which is an abstract model for autonomous vehicles. This paper presented an extended Kalman filter with the optimal linearization rate. Another major contributions of this paper was the presentation of a novel method for the estimation and stochastic control of nonlinear dynamic systems over the AWGN channel. It has been shown in this paper that the method, which is based on the linearization with the fixed rate, has lighter computational load; but it is not able to track fast reference signals. On the other hand, the method, which is based on the linearization with variable rate, is able to track both fast and slow reference signals; but it is computationally expensive. Hence, to track slow reference signals, the first method is recommended and for tracking fast reference signals, the second method is recommended.

Linearization at an operating point for strongly nonlinear or discontinuous dynamic is not a suitable method and the proposed technique is not applicable. In addition, the proposed technique, generally speaking, is computationally expensive. It requires frequent linearization at operating points and at each time instant the computation of the mean square estimation error at the encoder and decoder using the Monte Carlo. Hence, for future it is interesting to develop nonlinear estimation and control methods for controlling nonlinear systems over the AWGN channel in order to present less computationally expensive methods and particularly suitable for controlling strongly nonlinear or discontinuous systems over the AWGN channel. The nonlinear control and observer methods presented in [31] and [32] may be suitable candidates for this extension.

## REFERENCES

[1] Farhadi, A., Domun, J. and Canudas de Wit, C. (2015). A supervisory control policy over an acoustic communication network. *International Journal of Control*, 88(5), 946 - 958.

[2] Jadaan, K., Zeater, S. and Abukhalil, Y. (2017). Connected vehicles: An innovative transport technology, 187, 641 - 648.

[3] Nuno, E., Sarras, I. and Basanez, L. (2014). An adaptive controller for bilateral teleoperation: Variable time-delay case. *IFAC Proceedings*, 47(3): 9341 - 9346.

[4] Liu, C., Guo, J. and Pognet, P. (2018). Nonlinear model - mediated teleoperation for surgical applications under time variant communication delay. *IFAC Proceedings*, 51(22): 493 - 499.

[5] Yoshida, K. and Namerikawa, T. (2008). Predictive PD control for teleoperation with communication delay. *IFAC Proceedings*, 41(2): 12703 - 12708.

[6] Eusebi, A. and Melchiorri, C. (1998). Force reflecting telemanipulators with time-delay: Stability analysis and control design. *IEEE Transactions on Robotics and Automation*, 14(4): 635 - 640.

[7] Imaida, T., Yokokohji, Y., Doi, t., Oda, M. and Yoshikwa, T. (2004). Groundspace bilateral teleoperation of ETS-VII robot arm by direct bilateral coupling under 7-s time delay condition. *IEEE Transactions on Robotics and Automation*, 20(3): 499 - 511.

[8] Anderson, R. J. and Spong, M. W. (1998). Bilateral control of teleoperators with time delay. *Proceedings of the IEEE conference on Decision and Control*, 167 - 173.

[9] Charalambous, C. D., and Farhadi, A. (2008). LQG optimality and separation principle for general discrete time partially observed stochastic systems over finite capacity communication channels. *Automatica*, 44(12), 3181 - 3188.

[10] Parsa, A. and Farhadi, A. New coding scheme for the state estimation and reference tracking of nonlinear dynamic systems over the packet erasure channel (IoT): Applications in tele-operation of autonomous vehicles, *European Journal of Control*, 57, 242 - 252, April 2021.

[11] Farhadi, A. (2017). Sub-optimal control over AWGN communication network. *European Journal of Control*, 37, 27 - 33.

[12] Tatikonda, S. and Mitter, S. (2004). Control over noisy channels. *IEEE Trans. Autom. Control*, 49(7), 1196 - 1201.

[13] Braslavsky, J. H., Middleton, R. H. and Freudenberg, J. S. (2007). Feedback stabilization over signal-to-noise ratio constrained channels. *IEEE Trans. Autom. Control*, 52(8), 1391 - 1403.

[14] Li, Y., Chen, J., Tuncel, E. and Su, W. (2016). MIMO control over additive white noise channels: Stabilization and tracking by LTI controllers. *IEEE Transactions on Automatic Control*, 61(5), 1281 - 1296.

[15] Nair G. N., Evans R. J., Mareels I. M. Y., and Moran W. (2004). Topological feedback entropy and nonlinear stabilization. *IEEE Trans. Automat. Contr.*, 49(9), 1585 - 1597.

[16] S. D. Takloo, A. Farhadi and A. Khaki-Sedigh, "Control and Measurement of Nonlinear Dynamic Systems over AWGN Channel with Application in Tele-operation of Autonomous Vehicles," 2022 30th Mediterranean Conference on Control and Automation (MED), 2022, pp. 835-840, doi: 10.1109/MED54222.2022.9837145.

[17] Heemels W. P. M. H., Teel, A. R., Van de Wouw N., and Nescic, D. (2010). Networked control systems with communication constraints: Tradeoffs between transmission intervals, delays and performance. *IEEE Trans. Automat. Contr.*, 55(8), 1781 - 1796.

[18] Parsa A. and Farhadi, A. Tele-operation of autonomous vehicles over additive white Gaussian noise channel, *Scientia Iranica*, 1592-1605, Winter and Spring 2021.

[19] E. Nuno, I. Sarras and L. Basanez (2014). An adaptive controller for bilateral teleoperation: Variable time-delay case. *IFAC Proceedings*, 47(3): 9341 - 9346.

[20] R. J. Anderson and M. W. Spong Bilateral control of teleoperators with time delay. *Proceedings of the IEEE conference on Decision and Control*, 167 - 173 (1998).

[21] Sanjeroon, V., Farhadi, A., Motahari, A. and Khalaj, B. Estimation of nonlinear dynamic systems over communication channels. *IEEE Transactions on Automatic Control*, 63(9), 3024 - 3031 (2018).

[22] Parsa, A. and Farhadi, A. Measurement and control of nonlinear dynamic systems over the Internet (IoT): Applications in remote control of autonomous vehicles, *Automatica*, 95, 93 - 103, 2018.

[23] Slotine, J. J. and Li, W. (1991). *Applied Nonlinear Control*. Prentice-Hall.

[24] Gustafsson, F., Hendeby, G. (2012). Some relations between extended and unscented Kalman filters. *Signal Processing, IEEE Transactions on*, vol.60, no.2, 545 - 555.

[25] Lin, H. and Antsaklis, P. J. (2009). Stability and stabilizability of switched linear systems: A survey of recent results. *IEEE Transactions on Automatic Control*, 54(2), 308 - 322.

[26] Zhai, G. Hu, B., Yasuda, K. and Michel, A. N. (2002). Qualitative analysis of discrete-time switched systems. In *Proceedings of the American Control Conference*, (pp. 1880 - 1885).

[27] Caines, P.E. (2018). *Linear Stochastic Systems*. SIAM Publication.

[28] Reif, K., Gunther, S., Yaz, E. and Unbehauen, R. Stochastic stability of the discrete - time extended Kalman filter. *IEEE Trans. on Automatic Control*, 44(4), pp. 714 - 728.

[29] Kluge, S., Reif, K. and Brokate, M. Stochastic stability of the extended Kalman filter with intermittent observations. *IEEE Trans. on Automatic Control*, 55(2), pp. 514 - 518.

[30] Oriolo, G., De Luca, A. and Vendittelli, M. (2002). WMR control via dynamic feedback linearization: Design, implementation, and experimental validation. *IEEE Transactions on Control Systems Technology*, 10(6), 835 - 852.

- [31] Li, Y., Xu, N., Niu, B., Chang, Y. Zhao, J. and Zhao, X. (2021). Small-gain technique-based adaptive fuzzy command filtered control for uncertain nonlinear systems with unmodeled dynamics and disturbances. *Int. J. Adapt Control Signal Process*, pp. 1- 21.
- [32] Li, Y., Niu, B., Zong, G., Zhao, J. and Zhao, X. (2021). Command filter-based adaptive neural finite-time control for stochastic nonlinear systems with timevarying full-state constraints and asymmetric input saturation. *International Journal of System Science*,